Journal of Thermal Analysis and Calorimetry, Vol. 93 (2008) 1, 201–206

THERMAL PROPERTIES AND PHASE TRANSITIONS IN BLENDS OF NYLON-6 WITH SILK FIBROIN

H. Chen, X. Hu and Peggy Cebe[*]

Department of Physics and Astronomy, Tufts University, Medford, MA 02155, USA

The thermal and structural properties of binary blends of Nylon-6 (N6) and a chemically related biopolymer, *Bombyx mori* silk fibroin (SF), are reported in this work. Homopolymers and blends, in composition ratios of N6/SF ranging from 95/05 to 70/30, were investigated by thermogravimetric (TG) analysis, differential scanning calorimetry (DSC), Fourier transform infrared (FTIR) spectroscopy and wide angle X-ray scattering (WAXS). Silk fibroin typically degrades at temperatures just above 210°C, which occurs within the melting endotherm of N6. In TG studies, the measured mass remaining was slightly greater than expected, indicating the blends had improved thermal stability. No beta sheet crystals of SF were detected by FTIR analysis of the Amide I region.

Strong interaction between N6 and SF chains was observed, possibly as a result of formation of hydrogen bonds between N6 and SF chains. DSC analysis showed that the addition of SF to N6 caused a decrease in the crystallization temperature, the melting temperature of the lowest melting crystals and the crystallinity of N6. Furthermore, the α-crystallographic phase dominates and the γ-crystallographic phase was not observed in N6/SF blends, in contrast to the homopolymer N6, which contains both phases. We suggest that the addition of SF might result in changes of the chain extension of N6, which lead to the appearance of α- rather than γ-phase crystals.

Keywords: *binary blends, Nylon-6, silk fibroin, thermal stability*

Introduction

Nylon-6 (N6), a member of the polyamide group, is a commercially important engineering thermoplastic with good thermal and mechanical properties. The structure of semicrystalline N6 has been widely studied [1–5]. Depending upon thermal history, Nylon-6 crystallizes into two crystallographic forms: monoclinic α-phase and hexagonal/pseudohexagonal γ-phase. In general, fast cooling or quenching from the melt produces the γ-phase, while slow cooling yields α-phase [1–5]. γ-phase is unstable and will undergo cold crystallization at room temperature and transform to α-phase when heated up to about 150°C [5, 6]. The α phase is stable before melting.

Bombyx mori (domesticated silkworm) silk fibroin is a member of the nylon structural family and is considered to be chemically related to Nylon-2. Silk fibroin (SF) is a fibrous protein and is a candidate material for biotechnological and biomedical applications because it has several useful properties such as good biocompatibility, biodegradability and on a mass basis it is mechanically stronger than steel. The dynamic storage modulus of SF remained unchanged during heating up to 170°C [7]. SF has its glass transition temperature around 178°C and onset degradation temperature about 210°C [8, 9]. As a result of thermal degradation, β-sheet crystals of silk fibroin have never been observed to melt. To obtain even better mechanical and biomedical properties, natural SF polymer has been blended with other materials, such as chitosan [10], poly(acrylic acid) [11], poly(vinyl alcohol) [12], cellulose [13, 14] and gelatin [15] using a solution blending method.

Exposure of the aqueous solution of silk fibroin to organic solvents, mechanical stress, and/or thermal treatment can induce formation of the insoluble anti-parallel β-sheet secondary structure (called 'Silk II' [8, 9]) in degummed silk fibroin films. In the β-sheet secondary structure, hydrogen bonds form between the anti-parallel 'polyamide-like' chains [8, 9, 16–20]. The various side groups of the amino acids are perpendicular to the plane of the β-sheet. In comparison, in Nylon-6, for the α-crystallographic phase, hydrogen bonds form between anti-parallel polyamide chains, while for the γ-crystallographic phase, hydrogen bonds form between parallel polyamide chains [5]. Because of similarities in chemical structure, crystal structure and especially the pattern of hydrogen bond formation between Nylon-6 and silk fibroin, we anticipate that synergistic interaction might be possible where these materials formed into binary blends. However, until the present study, there have been no reports of blending of N6 and SF.

In the present work, we investigate the thermal and structural properties of N6/SF blends prepared from solution over a wide concentration range. We

* Author for correspondence: peggy.cebe@tufts.edu

1388–6150/$20.00

Akadémiai Kiadó, Budapest, Hungary
Springer, Dordrecht, The Netherlands

used thermogravimetric (TG) analysis, differential scanning calorimetry (DSC), Fourier transform infrared (FTIR) spectroscopy and X-ray scattering to determine the impact of blending on stability, crystallographic form and hydrogen bond formation. Strong interaction between N6 and SF chains was observed. Thermal properties of SF were improved by blending with N6. However, degree of crystallinity decreased and the crystals of N6 became less perfect with SF addition.

Experimental

Materials

Cocoons of *Bombyx mori* silkworm (obtained from Tsukuba, Japan), were boiled for 25 min in an aqueous solution of 0.02 M Na_2CO_3 and rinsed thoroughly with water to extract the glue-like sericin. The remaining silk fibroin was dissolved in a 9.3 M LiBr solution at 60°C for 4~6 h and then dialyzed in distilled water using a Slide-a-Lyzer dialysis cassette (Pierce, MWCO 3500) for 2 days. After centrifugation and filtration to remove insoluble residues, the final 2~5 mass% silk fibroin aqueous solution was cast in a polystyrene Petri dish to make the silk fibroin film. The fibroin films were then lyophilized and re-dissolved in hexafluoro-2-propanol (HFIP) to obtain a silk fibroin solution containing 5 mass% solids in HFIP.

Nylon-6 (resin grade 8082) was obtained from Honeywell in pellet form. Nylon-6 (N6) pellets were also dissolved separately in HFIP to obtain a Nylon-6 solution with 3 mass% solids in HFIP. N6/SF blends were prepared by mixing these stock solutions to achieve the following mass ratios of N6 to SF: 100/0, 95/5, 90/10, 85/15, 80/20, 75/25, 70/30 and 0/100. Films of the blends were cast from solution into Petri dishes and then dried in a vacuum oven at 110°C for several days to remove residual HFIP. The solutions and resulting dried blend films were optically transparent. Samples were kept in a desiccator to minimize moisture pick-up. DSC results confirmed that: 1) there was no plasticization of the blends by residual HFIP solvent and 2) homopolymer SF had no β-sheets after preparation from HFIP [8, 9].

Methods

FTIR measurements

Infrared absorbance spectra of all blends were collected using a Bruker Equinox 55 FTIR spectrometer in transmission mode. For each measurement, 64 scans were co-added with resolution 4 cm^{-1} in the wavenumber region of 400-4000 cm^{-1}.

TG measurements

The TA Q500 thermogravimetric analyzer was used to investigate the thermal degradation of the blends. The samples were scanned from room temperature to 600°C at a heating rate of 10°C min^{-1} in nitrogen atmosphere.

DSC measurements

DSC studies were carried out using TA Instruments temperature modulated DSC (TA Q100). Indium was employed for the temperature and heat flow calibration. The heat capacity was evaluated with respect to sapphire standard. Dry nitrogen gas was purged into the DSC cell with a flow rate of 50 mL min^{-1}. DSC measurements were performed at a heating rate of 5°C min^{-1}. For cooling scans, N6/SF blends were melted at 230°C for 3 min to erase prior thermal history and cooled at 20°C min^{-1}. Endotherms are presented with downward deflection in our scans. For the crystallinity measurements, a heat of fusion of ΔH_f=241 J g^{-1} was assumed for 100% crystalline Nylon-6 monoclinic α-phase [5]. The degree of crystallinity χ_C was obtained from:

$$\chi_C=\Delta H_f(\text{meas})/\Delta H_f \quad (1)$$

where ΔH_f(meas) is the measured heat of fusion.

X-ray scattering measurements

Wide-angle X-ray scattering (WAXS) patterns of N6/SF blends were obtained at room temperature on a Bruker AXS from 2θ=8–35° (for θ the half-scattering angle) at wavelength λ=0.1545 nm, using a 2-D gas filled wire detector. Scattered intensity was corrected for air background and the two-dimensional isotropic pattern was converted to a one-dimensional pattern by integrating over a sector.

Results and discussion

In order to examine the interaction between N6 chains and SF chains, FTIR was used to study the Amide groups of N6 and SF. Figure 1 shows the IR spectra of N6/SF blends in the Amide I region. N6 showed an absorption band at 1637 cm^{-1} (Amide I), attributed to the C=O stretching in N6. SF showed a broad absorption band at 1655 cm^{-1} (Amide I) attributed to the C=O stretching in SF. The SF spectrum is typical of a protein spectrum containing only random coils, side chains, α helices and turns secondary structures. For SF, the Amide I peak at 1655 cm^{-1} is assigned to the random-coil conformation and the Amide I peak will shift from 1655 to 1625 cm^{-1} if β-sheet conformation is formed [8, 15, 21–23]. For SF and N6/SF blends cast from HFIP solution, no apparent peak could be

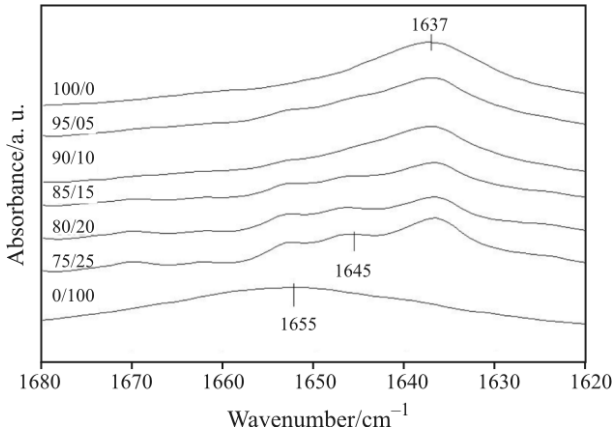

Fig. 1 FTIR absorbance *vs*. frequency in the Amide I region, for N6/SF blends cast from HFIP solution

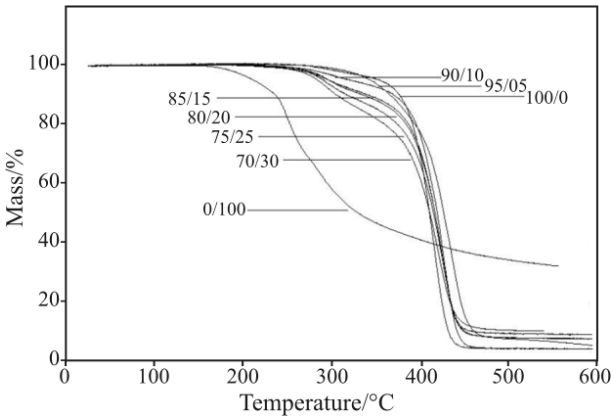

Fig. 2 Mass loss *vs*. temperature for N6/SF blends, cast from HFIP solution

observed at 1625 cm^{-1}, indicating that no β-sheet secondary structures (i.e., no crystals) were formed in either SF or N6/SF blends cast from HFIP.

In N6/SF blends, the Amide I peaks of N6 and SF homopolymers still could be observed and a new absorption band at about 1645 cm^{-1} was also observed in all blended samples. This band could be related to the interaction between N6 and SF chains. Some hydrogen bonds might be formed between N6 chains and SF chains, resulting in a new vibration of C=O stretching in the N6/SF blends. Appearance of new hydrogen bonds between N6 and SF will affect the vibrations of the C=O bonds and therefore will be seen as a change in Amide I region. Since the Amide II absorbance bands of N6 (1543 cm^{-1}) and SF (1545 cm^{-1}) are very close, it is difficult to discuss the interaction between SF and N6 in this region and the same situation occurs with the Amide III region.

Usually, strong interaction between blend components will improve the thermal stability of the blends [24]. Thermogravimetric analysis results of N6, SF and N6/SF blends are shown in Fig. 2. Silk fibroin homopolymer, 0/100, shows mass loss beginning at about 170°C; above 230°C, thermal degradation begins. N6 homopolymer, 100/0, is stable to a higher temperature than SF. For example, at 260°C, N6 has lost no mass, whereas SF has lost 25% of its mass. Results of mass loss during heating are presented in Table 1.

Table 1 shows the expected, M_E, and measured, M_M, mass remaining in N6/SF blends at the indicated temperatures (230, 260, 300 and 350°C), expressed as a percentage of the initial mass. The expected mass remaining at temperature T, $M_E(T)$, indicates the behavior of a non-interacting mixture of two components. On this assumption, of no synergism between the two components, $M_E(T)$ is calculated from:

$$M_E(T)=M_{N6}(T)\Phi_{N6}+M_{SF}(T)(1-\Phi_{N6}) \qquad (2)$$

where $M_{N6}(T)$ and $M_{SF}(T)$ are the measured masses remaining at temperature T, for N6 and SF, respectively; and Φ_{N6} is the mass fraction of N6 in the N6/SF blends. The measured mass remaining in the N6/SF blends is always larger than the expected mass remaining at the selected temperatures. This indicates

Table 1 Expected (E) and measured (M) mass remaining at various temperatures and degree of crystallinity of N6/SF blends[#]

N6/SF	M_E 230°C/%	M_M 230°C/%	M_E 260°C/%	M_M 260°C/%	M_E 300°C/%	M_M 300°C/%	M_E 350°C/%	M_M 350°C/%	χ_C[a]±0.01	λ_C^N[b]±0.01
100/0	100	100	100	100	98.8	98.8	93.6	93.6	0.30	0.30
95/05	99.6	100	98.8	100	96.7	98.5	91.2	95.6	0.30	0.32
90/10	99.2	100	97.5	99.3	94.7	96.6	88.9	92.9	0.28	0.31
85/15	98.8	100	96.3	98.9	92.7	94.8	86.5	89.2	0.28	0.33
80/20	98.3	100	95.0	99.3	90.6	94.7	84.1	88.5	0.27	0.34
75/25	97.9	100	93.8	98.9	88.6	93.2	81.8	85.7	0.26	0.35
70/30	97.5	100	93.5	98.6	86.6	91.5	79.4	82.4	0.25	0.36
0/100	91.7	91.7	75.0	75.0	58.0	58.0	46.3	46.3	0	0

#Blends were prepared from HFIP solution. [a]χ_C is obtained from the heat of fusion by using Eq. (1). [b]χ_C^N is the normalized crystallinity of N6 from $\chi_C^N=\chi_C/\Phi_{N6}$

that there is a positive synergistic effect of blending on the thermal mass loss of the N6/SF blends.

From Fig. 2, a two-step mass loss mechanism is observed in the N6/SF blends. The first step of the mass loss is related to the degradation of SF and occurs at lower temperature; the second step of the mass loss is due to degradation of N6 and occurs at higher temperature. The onset temperature of the thermal decomposition of the blends is higher than that of SF homopolymer and increases with an increase in content of N6. These results may indicate that the formation of hydrogen bonds between N6 and SF can stabilize SF when it appears in binary blends with a chemically related polymer.

Normalized heat flow *vs*. temperature results are shown in Fig. 3, for different compositions of N6/SF blends cast from HFIP solution and scanned at 5°C min^{-1} from 0°C to above the melting point of the N6 crystals. The curves are presented with the same scaling, but are displaced vertically for clarity. The heat flow has been normalized for total sample mass. The glass transition of the N6 component of the blends was observed between 40 and 55°C, but is not apparent in Fig. 3 due to the vertical scaling. The glass transition of homopolymer SF is around 178°C, which is close to the onset melting point of N6 crystals, but is also not observable in Fig. 3 because of the vertical scaling. There was no glass transition for SF observed in the blends. One possible reason is that the glass transition of SF is hidden within the melting region of N6. Another is that the blends are miscible and only a single glass transition could be observed.

The treatment used to create the blends from solution did not introduce any β-sheet crystals of SF, nor was there any cold-crystallization exotherm of β-sheet crystals observed between the glass transition temperature and 200°C, where such a feature is observed in the homopolymer SF [9]. We conclude that the strong interaction between SF and N6 prevents the SF from crystallizing. Furthermore, there should be no large pockets of un-crystallized SF phase separated from the Nylon-6, since such pockets would be likely to transform from random coil to β-sheet crystals during heating. It would be interesting for additional studies to be conducted on blends with larger SF content, to determine at what composition of SF the β-sheet crystals form.

Above 200°C, multiple-melting peaks are observed for all the N6/SF blends. The lower melting peak, T_{m1}, is due to the melting of original crystals of N6. The upper melting peak, T_{m2}, is due to the melting of crystals that either re-crystallized or reorganized during heating after melting of the original crystals. T_{m1} shifted to lower temperature while T_{m2} remained constant with an increase of SF. Values of T_{m1} and T_{m2} are shown in Table 2. The normalized crystallinity, χ_C, of N6 in N6/SF blends, is shown in the last column of Table 1; χ_C increases slightly with an increase of SF content. Furthermore, an endotherm peak due to the degradation of SF is observed above 250°C in Fig. 3, consistent with the observation from TG analysis.

Another explanation for the enhanced thermal stability of SF could be the presence of N6 crystals. From Figs 2 and 3, we observe that N6 starts to melt at about 200°C, close to the temperature where the pure SF starts to degrade. These crystals might act to absorb the heat energy through unfolding the crystalline lamellae or break-up of the N6 crystalline fraction, re-

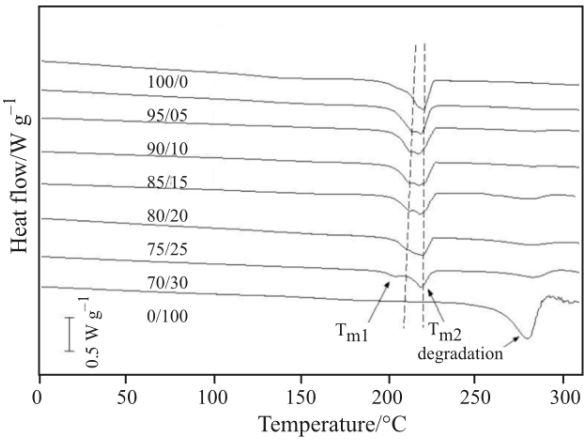

Fig. 3 Heat flow *vs*. temperature of N6/SF blends, cast from HFIP solution, during DSC heating at 5°C min^{-1}. Curves are displaced vertically for clarity

Table 2 Melting temperature and crystallization temperature of N6/SF blends

N6/SF	T_{m1}[a]/°C, ±0.1	T_{m2}[a]/°C, ±0.1	T_c[b]/°C, ±0.1	T_{m1}[b]/°C, ±0.1	T_{m2}[b]/°C, ±0.1
100/0	216.2	218.5	185.9	211.6	219.3
95/05	216.2	218.3	185.6	209.8	219.2
90/10	212.5	218.2	185.3	209.2	219.2
85/15	211.8	218.1	184.3	210.1	219.1
80/20	211.4	218.1	184.0	208.4	218.6
75/25	210.6	218.0	183.7	208.2	218.0

[a]Samples cast from HFIP solution. [b]Samples prepared by cooling from the melt

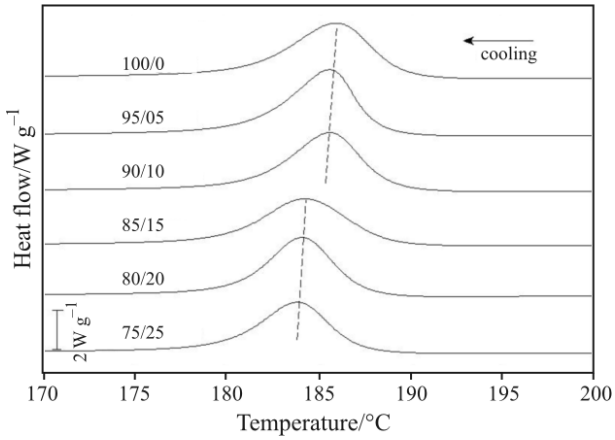

Fig. 4 Heat flow *vs*. temperature of N6/SF blends, cast from HFIP solution, during DSC cooling from the melt at 20°C min^{-1}. Curves are displaced vertically for clarity

sulting in an increase of the degradation temperature of SF after the melting the N6.

Figure 4 shows the DSC results of N6/SF blends during cooling. The crystallization temperature of N6/SF blends slightly decreases and the normalized crystallinity of N6 of N6/SF blends, obtained from the area of the crystallization exotherm during cooling, increases modestly with SF addition from 0.27 for N6/SF 100/0 to 0.31 for N6/SF 75/25.

Figure 5 shows the normalized heat flow *vs*. temperature for different compositions of N6/SF blends during heating after cooling from the melt, which provides a uniform thermal history to the blends. The curves are presented with the same scaling, but are displaced vertically for clarity. The heat flow has been normalized for total sample mass. Multiple-melting peaks are observed for N6/SF blends during the second heating. T_{m1} shifts to lower temperature and T_{m2} remained almost constant with an increase of SF content, similar to the thermal behavior of the solution-cast blends. Regardless of whether the blends come directly from solution or are treated by cooling from the melt, original crystals of N6 will become less perfect with SF addition, resulting in the decrease of T_{m1}. But the recrystallization or reorganization of N6 crystals was not strongly affected by SF addition, as signified by no apparent change of T_{m2}.

X-ray results for N6/SF blends after cooling from the melt at 20°C min^{-1} are shown in Fig. 6. For homopolymer N6, both α- and γ-crystallographic phases were observed. However, with an increase of SF, only the α-crystalline phase was observed. The overall N6 crystallinity, determined from the ratio between the crystalline peaks and the total area of coherent scattering [25], in the blends decreases as SF content increases. For the blends cast from solution, only the α-crystallographic phase could be observed for all compositions and these results are not presented in the interests of brevity.

To reach the maximization level of hydrogen bonding in the crystalline state of N6, chains of N6 need to adopt either extended or twisted configurations [5]. The fully extended configuration results in α-crystallographic phase, where the carbonyl and nitrogen–hydrogen groups are located in the plane of the anti-parallel chains (CH_2 zigzags). For the twisted configuration, termed the γ-phase, the carbonyl and nitrogen–hydrogen groups are not fully extended and are located out of the plane of the chains. The preference for N6 to crystalline in α- or γ-phase has been observed in different filled N6 composites. In the carbon black/N6, titanium dioxide/N6 and $FeCl_3$/N6 composites, α-phase is more dominant relative to γ-phase [26, 27]. In the kaolin/N6 composites, γ-phase is dominant [26]. Generally, in N6 nanocomposites, the presence of clay will enhance the formation of γ-phase

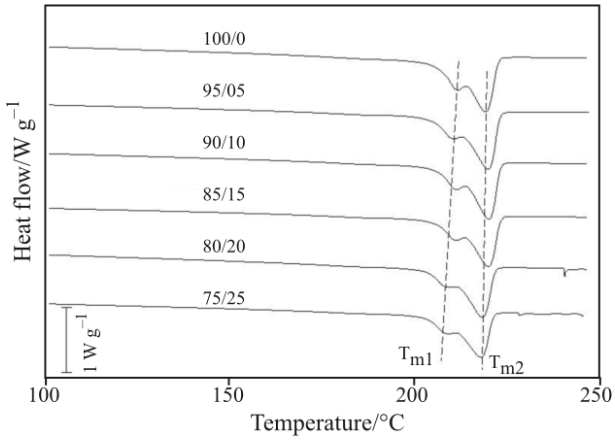

Fig. 5 Heat flow *vs*. temperature of N6/SF blends, prepared by cooling from the melt, during reheating at 5°C min^{-1}. Curves are displaced vertically for clarity

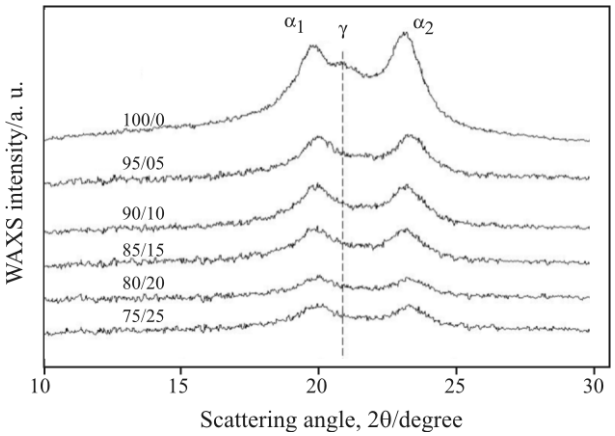

Fig. 6 Wide-angle X-ray scattering intensity *vs*. scattering angle, for N6/SF blends. Blends were prepared by cooling from the melt at 20°C min^{-1}. Scans were taken at room temperature. The characteristic reflections of the N6 α- and γ-crystallographic phases are indicated

[5, 28–30]. The popular explanation is that the clay will force the amide groups out of the plane formed by chains [28–30]. For the N6/SF blends treated by cooling from the melt, the preference to form α-phase upon SF addition, could be similarly related to the degree of chain extension. SF might extend the chains of N6 and force the amide group into the plane of the chains, resulting in the formation of the fully-extended α-crystalline phase.

Conclusions

Due to similarities of chemical structure between N6 and SF, strong interaction between these two-blend partners has been observed. Combining DSC with TG measurements showed that thermal stability of SF was improved by adding N6 and increased with an increase of N6 content. This could be due to the presence of hydrogen bonds between the chains of SF and N6, and/or the presence of N6 crystals. T_{m1} values were steadily depressed and T_{m2} remains almost constant with an increase of SF content for the blends prepared either from solution or by cooling from melt. This indicates the original N6 crystals became less perfect with SF addition. Crystallization temperatures of N6 were slightly depressed and the degree of crystallinity was decreased, with an increase of SF content. Although homopolymer N6 exhibits both α- and γ-crystallographic phases, in the N6/SF blends only α-phase was observed. The addition of SF might result in changes of the chain extension of N6, which lead to the appearance of α-phase and absence of γ-phase.

Acknowledgements

The authors thank the National Science Foundation for support of this work through the Polymers Program of the Division of Materials Research under DMR-0602473 and the MRI Program under DMR-0520655 for thermal analysis instrumentation.

References

1 K. H. Illers and H. Haberkorn, Makromol. Chem., 142 (1971) 31.
2 M. Kyotani and S. Mitsuhashi, J. Polym. Sci., Part A-2, 10 (1972) 1497.
3 N. S. Murthy, S. A. Curran, S. M. Aharoni and H. Minor, Macromolecules, 24 (1991) 3215.
4 I. Campoy, M. A. Gomez and C. Marco, Polymer, 39 (1998) 6279.
5 T. D. Fornes and D. R. Paul, Polymer, 44 (2003) 3945.
6 S. S. Pesetskii, B. Jurkowski, Y. A. Olkhov, S. P. Bogdanovich and V. N. Koval, Eur. Polym. J., 41 (2005) 1380.
7 M. Tsukada, G. Freddi, M. Nagura, H. Ishikawa and N. Kasai, J. Appl. Polym. Sci., 46 (1992) 1945.
8 X. Hu, D. Kaplan and P. Cebe, Macromolecules, 39 (2006) 6161.
9 X. Hu, D. Kaplan and P. Cebe, Thermochim. Acta, 461 (2007) 137.
10 H. Y. Kweon, I. C. Um and Y. H. Park, Polymer, 42 (2001) 6651.
11 Q. W. Gao, Z. Z. Shao, Y. Y. Sun, H. Lin, P. Zhou and T. Y. Yu, Polymer J., 32 (2000) 269.
12 K. Yamaura, N. Kuranuk, M. Suzuki, T. Tanigami and S. Matsuzawa, J. Appl. Polym. Sci., 41 (1990) 2409.
13 G. Yang, L. N. Zhang and Y. G. Liu, J. Membr. Sci., 177 (2000) 153.
14 E. S. Sashina, G. Janowska, M. Zaborski and A. V. Vnuchkin, J. Therm. Anal. Cal., 89 (2007) 887.
15 E. S. Gil, D. J. Frankowski, M. K. Bowman, A. O. Gozen, S. M. Hudson and R. J. Spontak, Biomacromolecules, 7 (2006) 728.
16 M. Ishida, T. Asakura, M. Yokoi and H. Saito, Macromolecules, 23 (1990) 88.
17 X. Chen, D. P. Knight, Z. Z. Shao and F. Vollrath, Polymer, 42 (2001) 9969.
18 A. Motta, L. Fambri and C. Migliaresi, Macromol. Chem. Phys., 203 (2002) 1658.
19 N. Agarwal, D. A. Hoagland and R. J. Farris, J. Appl. Polym. Sci., 63 (1997) 401.
20 O. N. Tretinnikov and Y. Tamada, Langmuir, 17 (2001) 7406.
21 E. Goormaghtigh, V. Cabiaux and J. M. Ruysschaert, Eur. J. Biochem., 193 (1990) 409.
22 C. Jung, J. Mol. Recognit., 13 (2000) 325.
23 A. Dong, P. Huang and W. S. Caughey, Biochemistry, 29 (1990) 3303.
24 Y. Nishio and R. S. Manley, Macromolecules, 21 (1988) 1270.
25 H. Chen and P. Cebe, J. Therm. Anal. Cal., 89 (2007) 417.
26 T. Kyu, Z. L. Zhou, G.C. Zhu, Y. Tajuddin and S. Qutubuddin, J. Polym. Sci., Part B, 34 (1996) 1761.
27 V. M. Cheshkov, M. M. Natova, N. R. Ashurov, M. M. Usmanova and A. M. Vekselman, Eur. Polym. J., 27 (1991) 205.
28 D. M. Lincoln, R. A. Vaia, Z. G. Wang and B. S. Hsiao, Polymer, 42 (2001) 1621.
29 X. Liu and Q. Wu, Polymer, 43 (2002) 1933.
30 Q. Wu, X. Liu and L. A. Berglund, Polymer, 43 (2002) 2005.

DOI: 10.1007/s10973-007-8885-y